Variability of Storm-Relative Helicity during VORTEX

PAUL M. MARKOWSKI AND JERRY M. STRAKA

School of Meteorology, University of Oklahoma, Norman, Oklahoma

ERIK N. RASMUSSEN AND DAVID O. BLANCHARD

Cooperative Institute for Mesoscale Meteorological Studies, National Severe Storms Laboratory, Boulder, Colorado

ABSTRACT

In this paper, storm-relative helicity (SRH) and low-level vertical shear of the horizontal wind fields were investigated on the mesoscale and stormscale in regions where tornadoes occurred for four case studies using data collected during the Verification of the Origin of Rotation in Tornadoes Experiment. A primary finding was that SRH was highly variable in both time and space in all of the cases, suggesting that this parameter might be difficult to use to predict which storms might become tornadic given the available National Weather Service upper-air wind data. Second, it was also found that the shear between the lowest mean 500-m wind and the 6-km wind was fairly uniform over vast regions in all of the four cases studied; thus, this parameter provided little guidance other than that there was possibly enough shear to support supercells. It was contended that forecasters will need to monitor low-level features, such as boundaries or wind accelerations, which might augment streamwise vorticity ingested into storms. Finally, it was suggested that one reason why one storm might produce a tornado while a nearby one does not might be due to the large variations in SRH on very small spatial and temporal scales. In other words, only those storms that move into regions, small or large, with sufficient SRH might produce tornadoes.

1. Introduction

Typically, only standard, 12-hourly National Weather Service (NWS) rawinsonde, 5-min NWS WSR-88D Doppler radar velocity azimuth displays (VAD), and 6-min to hourly profiler upper-air data are available to evaluate wind-derived parameters for severe storm forecasts. Unfortunately, profiler data generally are poor quality in the lower levels [0–1.5 km above ground level (AGL); Richardson 1993; D. Burgess and F. Carr 1997, personal communication] and VAD data are poor in the upper levels (D. Burgess and D. Zrnić 1997, personal communication), which limits use of these platforms. Moreover, rawinsondes also have to be interpreted with care as they may travel more than 100 km before reaching the tropopause.

In forecasting the most severe convective storms, which also tend to be those that are long lasting and rotating, parameters such as the bulk Richardson number (Weisman and Klemp 1982, 1984), 0–4-km shear (Rasmussen and Wilhelmson 1983), and storm-relative environmental helicity (SREH, described in the next sec-

tion; Davies-Jones 1984, 1993; Lilly 1986a,b; Davies-Jones et al. 1990; Davies and Johns 1993; Johns et al. 1993) have been used. These parameters gained acceptance in practical applications in part through theoretical (Davies-Jones 1984; Lilly 1986a,b), numerical model (Brooks and Wilhelmson 1990; Brooks et al. 1993; Droegemeier et al. 1993), and observational (Leftwich 1990; Davies and Johns 1993; Johns et al. 1993; Hales and Vescio 1996) studies. Some of these studies demonstrated a high positive correlation between vertical vorticity and updrafts in convective storms occurring in environments with particular wind speed and direction morphology. As is well documented throughout the literature, storms developing in environments with large values of low-level shear and/or SREH are known to have a propensity for violent weather phenomena such as large hail, strong winds, and tornadoes.

Davies-Jones et al. (1990) and Davies-Jones (1993) showed changes of SREH by an order of magnitude on spatial scales of less than 100 km and temporal scales of less than 3 h (Fig. 1; from Davies-Jones 1993) in severe convective storm environments. Davies-Jones further suggested that rapid local changes in SREH could make tornado forecasting difficult. It is important to note that significant tornadoes have been highly associated with large values of resolved helicity (Rasmussen 1998, manuscript submitted to *Wea. Forecast-*
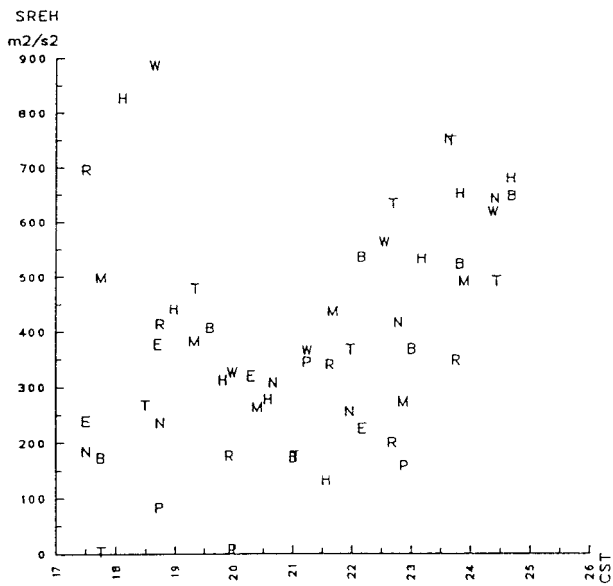
FIG. 1. SREH vs time on 29 April 1979 (storm motion 19 m s^{-1} from 233°). Letters identify stations (H = Chickasha, B = Blanchard, N = Noble, M = Minco, W = Wheatland, T = Tinker Air Force Base, R = El Reno, P = Piedmont, and E = Edmond; all are in Oklahoma). The spatial separation of all the stations is less than 100 km (from Davies-Jones 1993).

TABLE 1. Climatology of storm characteristics [nonsupercell (no hail, no tornadoes), supercell (hail > 2 cm, tornado ≤ F1), tornadic (tornado > F1)] based on SRH from proximity soundings as described by Rasmussen (1998, manuscript submitted to *Mon. Wea. Rev.*).

Category	Percentile				
	10	25	50	75	90
Nonsupercell	−12	−1	26	65	148
Supercell	−3	30	102	163	260
Tornadic	33	106	213	323	446

(CLASS; Lauritsen et al. 1987; Rust et al. 1990) sounding facilities (Rasmussen et al. 1994) and 3-hourly rawinsondes from selected NWS sites. In this paper it is shown that the inclusion of additional upper-air data collected by VORTEX in the analyses of the regular NWS upper-air data indicates more variability in helicity (in at least the tornadic environments investigated thus far) from that possibly detectable from the regularly available NWS upper-air wind data. Moreover, the results demonstrate that helicity varies over spatial and temporal scales that are essentially impossible to feasibly measure (and probably to numerically predict) with current technology. It is not known yet if this variability exists in more quiescent atmospheres or is found more often in association with atmospheres supportive of severe storms. Given this, the understanding of the possible causes and effects of this variability is difficult to define and therefore the severe weather forecast problem is probably compounded. Note that it is not the intent of this paper to explain these causes and effects in the cases studied, since the data collected thus far are too limited to draw firm conclusions, as has been the case for most previous similar studies.

In the past it has been common to use the term SREH. The use of the word "environment" makes the definition of SREH ambiguous, thus the term storm-relative helicity (SRH) is adopted, in general, hereafter. In this paper a description of SRH is presented in section 2; four case studies are presented in section 3 to demonstrate SRH variability; a discussion and summary of the present work and a mention of possible future work are presented in section 4.

2. Storm-relative helicity

The essence of SRH is described in some detail below. In addition the magnitude of the terms describing the generation of streamwise vorticity (from which SRH is derived) are put into perspective before describing the case studies. Helicity is a quantity derived from the streamwise vorticity (vorticity vector aligned with the velocity vector; Davies-Jones 1984). In a storm-relative framework, storm-relative helicity is

$$\text{SRH} = \int_0^H (\mathbf{v} - \mathbf{c}) \cdot \boldsymbol{\omega} \, dz, \qquad (1)$$

ing) as shown in Table 1 (from Rasmussen 1998, manuscript submitted to *Wea. Forecasting*). This has also been shown in other studies [e.g., Davies-Jones 1993; Davies and Johns 1993 and Johns et al. 1993; though it is not known if this is always the case, such as when convective available potential energy (CAPE) is very large; e.g., CAPE > 4000 J kg^{-1}]. It also is important to note that it is possible that only certain supercells in a given environment become tornadic by moving into regions with large values of helicity that might be unresolved owing to large variability in helicity (Richardson et al. 1998, manuscript submitted to *Mon. Wea. Rev.*) and as documented herein and by Davies-Jones et al. (1990) and Davies-Jones (1993). In other studies, Rasmussen and Wilhelmson (1983) and Maddox (1993) noted diurnal variations of 0–4-km shear and SREH, respectively, over the Great Plains of the United States. Maddox further suggested that the variations might be associated with diurnal oscillations of the low-level jet, which might play an important role in nocturnal tornado outbreaks. Finally, Brooks et al. (1994) demonstrated dramatic changes in SREH in the near environments of storms and that these owed to changes caused by inflow enhancement by the storms.

During 1994 and 1995 the Verification of the Origins of Rotation in Tornadoes Experiment (VORTEX; Rasmussen et al. 1994) took place over the south-central Plains with the goal of gaining a better understanding of tornadoes and their near environments. Additional upper-air information was available from nine Cross-chain Loran Atmospheric Sounding System-type

where $\mathbf{v} - \mathbf{c}$ is the storm-relative wind (environmental wind vector $\mathbf{v}$ minus the storm motion vector $\mathbf{c}$), and $\boldsymbol{\omega}_h$ is the horizontal vorticity vector defined here as

$$\boldsymbol{\omega}_h = \left(\frac{\partial w}{\partial y} - \frac{\partial v}{\partial z}, \frac{\partial u}{\partial z} - \frac{\partial w}{\partial x} \right), \qquad (2)$$

with u, v, and w the wind components and x, y, and z the components of the Cartesian coordinate system.

Assuming we are in the low levels (0–3 km) of an environment that would support rotating storms, a typical value that might be expected for $\Delta w/\Delta x$ or $\Delta w/\Delta y$ might be 1 m s^{-1}/10^4 m or about 10^{-4} s^{-1} (conceivably this could be as large as 10^{-3} s^{-1} at a boundary). In comparison, $\Delta u/\Delta z$ or $\Delta v/\Delta z$ might be 10 m s^{-1}/10^3 m or about 10^{-2} s^{-1} or possibly larger. Thus, the equation for $\boldsymbol{\omega}_h$ probably can be approximated as

$$\boldsymbol{\omega}_h = \left(-\frac{\partial v}{\partial z}, \frac{\partial u}{\partial z} \right), \qquad (3)$$

which shows that the horizontal vorticity vector is dominated by the vertical shear of the horizontal wind. The streamwise horizontal vorticity is defined as $(\mathbf{v} - \mathbf{c}) \cdot \boldsymbol{\omega}_h$. The integral in (1) is over the storm inflow depth H, often chosen to be 3 km AGL, approximately the level of free convection (Davies-Jones 1984). (Hereafter 0–3-km helicity is implied everywhere helicity is discussed.) SRH can be graphically computed as minus twice the area swept out by the storm-relative wind between 0 and H on a hodograph (Davies-Jones et al. 1990). By standard geometric convention, the area is negative (positive) if swept out clockwise (counterclockwise).

Storm-relative helicity is defined by the vertical integral of the dot product of the storm-relative wind and streamwise vorticity. The streamwise vorticity equation in natural coordinates can be written as

$$\frac{d\omega_s}{dt} = \omega_s \frac{\partial v}{\partial s} + \omega_n \frac{\partial v}{\partial n} + \omega_z \frac{\partial v}{\partial z} + \frac{\partial B}{\partial n} + F, \qquad (4)$$

where ω_s is the streamwise component of vorticity; ω_n is the crosswise component of vorticity; ω_z is the vertical component of vorticity; v is the flow along a streamline (scale defined by notation U); $B = g\Delta\theta_v/\theta_v$ is buoyancy [where B is buoyancy, g is gravity, θ_v is virtual potential temperature (no precipitation), and $\Delta\theta_v$ is virtual potential temperature perturbation]; s is the streamwise direction, n is the crosswise (normal, and positive to the left of the flow, by convention) direction (scale of s and n defined by notation L), z is the vertical component (scale defined by notation H); and F is friction (molecular-scale friction is assumed to be negligible). From a scale analysis of this equation, assuming the case of the environment on the storm scale ($L = 10^4$ m, $H = 10^3$ m, $U = 10$ m s^{-1}, $\Delta\theta_r = 5°$C, $\omega_{s,n} = 1.0 \times 10^{-2}$ s^{-1}, $\omega_z = 1.0 \times 10^{-3}$ s^{-1} to 1.0×10^{-4} s^{-1}), there is some confidence that dominant production mechanisms

for SRH are most likely to be baroclinic generation and horizontal stretching with an order of magnitude of about 10^{-3} s^{-1}. The vertical derivative term is about an order of magnitude smaller. Assuming an eddy mixing coefficient of about 100 m^2 s^{-1} in a well-mixed boundary layer, the eddy mixing term is smaller by a magnitude or more than that for the buoyancy and stretching terms. This would permit streamwise vorticity generated by a thermal boundary to exist possibly several hours after the buoyancy gradient dissipated.

The importance of boundaries in the problem described in this paper is baroclinic generation of vorticity related to temperature gradients (e.g., Klemp and Rotunno 1983; Rotunno et al. 1988). As temperature, or more accurately, buoyancy gradients often form in regions with a base motion normal to the gradient vector (i.e., flow parallel to the boundary; e.g., Maddox et al. 1980; Rotunno 1993; Richardson et al. 1998, manuscript submitted to *Mon. Wea. Rev.*), the baroclinically generated horizontal vorticity usually will be substantially streamwise:

$$\frac{d\omega_s}{dt} = \frac{\partial B}{\partial n} \qquad (5)$$

(as opposed to crosswise). Furthermore, longer residence times of a parcel in a barocline lead to greater amounts of horizontal vorticity. Values of horizontal vorticities associated with boundaries of 10^{-3} s^{-1}–10^{-2} s^{-1} probably are common (e.g., simple scale analysis; using $\Delta\theta_v = 1°$C–10°C and L = 10^4 m, see also Richardson et al. 1998, manuscript submitted to *Mon. Wea. Rev.*). The boundaries that might be considered include fronts on the synoptic scale or mesoscale, active or decaying thunderstorm outflows, sea breezes or inland sea breezes, or other boundaries (e.g., Purdom 1976, 1993; Maddox et al. 1980; Weaver and Nelson 1982; Rotunno and Klemp 1982; Weisman and Klemp 1984; Klemp and Rotunno 1983; Rotunno et al. 1988; Ziegler et al. 1995)

Finally, SRH may vary substantially near storms owing to the updraft of a storm. The low-level winds may be altered and strengthened as the parcel approaches an updraft that might stretch preexisting horizontal vorticity. The rate at which streamwise horizontal vorticity is increased owing to inflow accelerations/stretching is

$$\frac{d\omega_s}{dt} = \omega_s \frac{\partial v}{\partial s}, \qquad (6)$$

where ω_s, v, and s are as defined before. For a parcel that accelerates 10 m s^{-1} over a 40 km distance toward an updraft, ω_s can double in 45 min. According to Davies-Jones and Brooks (1993), cloud model results show that as the streamwise component is increased through stretching, SRH also will increase. Similarly, Bluestein et al. (1988) observed accelerations from 10–19 m s^{-1} in the surface to 2-km-AGL layer between the wall cloud and a point 125 km distant from the updraft base.

SRH approximately tripled along the path to that up-draft. It should be noted that horizontal stretching of streamwise vorticity occurs with all storms if SRH is present, not just tornadic ones.

3. Case studies

The analyses presented herein include upper-air data from standard NWS rawinsonde sites and times as well as data from nine CLASS rawinsondes (four fixed and five mobile). Also available were 3-hourly NWS rawinsonde data in the forecast target region. Surface data included that available from the NWS, Oklahoma Mesonet (Brock et al. 1995), ARM-CART sites (e.g., see Rasmussen et al. 1995), profiler sites, and 12 mobile mesonets (e.g., Straka et al. 1996; Rasmussen et al. 1994, 1995). Errors for NWS and M-CLASS winds are less than 1 m s^{-1} (e.g., Rasmussen et al. 1995), whereas those for profilers and VADs are about 1 m s^{-1} (D. Zrnić 1997, personal communication). The mobile mesonet errors are similar to those for the Oklahoma Mesonet (Brock et al. 1995; Straka et al. 1996). A summary of the errors associated with all of the VORTEX instruments is provided in Rasmussen et al. (1995).

In preparing the upper-air data, the NWS and M-CLASS rawinsonde winds were sampled to give the same resolution as that of the profiler data to avoid resolution biases (i.e., the NWS soundings contain more information). Values of SRH and the shear between the lowest mean 500-m wind and the 6-km wind were plotted on mesoscale maps and insets in regions where tornadic storms occurred. Storm motions for SRH were based on (a) 60% of the 0–4 km shear vector and 8 m s^{-1} to the right of it (Rasmussen 1998, manuscript submitted to *Wea. Forecasting*) for mesoscale maps, and (b) the average supercell motions observed on the inset maps. Since these values may not always be appropriate for each storm, sensitivity tests were performed to see how values of SRH might vary. The values can be considered accurate to within ±10–30 m² s^{-2}. Finally it is noted that values of SRH were not contoured. As will become apparent, doing so would be nearly impossible owing to the huge variability observed in many areas, and the fact that there are too few data points to make meaningful analyses.

a. 16–17 May 1995

During the afternoon and evening of 16–17 May 1995, supercells produced four tornadoes, ranging in intensity from F0 to F3, in a corridor from just east of Garden City, Kansas, to 80 km northeast of Dodge City, Kansas. Convection was initiated near 2200 UTC at the intersection of a dryline and subsynoptic trough west of Garden City, Kansas. The surface analysis for 2300 UTC shows an outflow boundary produced by previous convection. The position was delineated using satellite, radar, and surface observations using NWS and mobile

mesonet data. Aloft, a strong jet maximum propagated east-northeastward across southern Kansas and northern Oklahoma (bold arrow shows wind maximum within ±100–200 km; Fig. 2b) in association with the approaching shortwave.

Values of SRH from standard NWS rawinsonde and profiler sites over the southern Plains (defined hereafter as extreme eastern New Mexico, southeastern Colorado, Kansas, Oklahoma, and northern Texas) varied over an order of magnitude (Fig. 3a), with the largest values at Neodesha, Kansas (values from Haviland, Kansas, were not available owing to earlier lightning damage). Note the large variations over short distances (50–100 km) such as between the rawinsonde site in Norman, Oklahoma, and the profiler site in Purcell, Oklahoma. Similarly there are large variations in SRH in northwestern Oklahoma and southwestern Kansas between observation sites.

Focusing on the northwestern Oklahoma and southwestern Kansas area, values of SRH ranged from 9 to 284 m² s^{-2} using all data at all sites available. Sites in Kansas, where there were many boundaries (after 2300 UTC and therefore not shown in Fig. 2a) and numerous convective storms, show that some locations experienced dramatic temporal changes in SRH (Fig. 3b). Moreover, SRH varied on scales less than 50–100 km by at least an order of magnitude. The tornadoes did not necessarily occur near the largest values of observed SRH (though the values of SRH in the storms' near environments could never be determined). Values of SRH in northern Oklahoma were more homogeneous in time and space in this time–space window. In contrast to the variability of SRH, the shear values, as defined above, show smaller variability over the southern Plains, including the region of interest (Figs. 4a and 4b). In general, values computed become more supportive (larger) of supercells with time.

b. 17–18 May 1995

On 17–18 May 1995 a pair of shallow (echo tops <12 km) supercells produced tornadoes (one was an F2 20-km-track tornado; Fig. 5a) in northwest Oklahoma. Though not intercepted by VORTEX, the Oklahoma mesonet data showed that these storms were initiated near a surface low and moved parallel to a west–east thermal boundary. Aloft, a strong jet maximum propagated across central Oklahoma (Fig. 5b) during the day in association with the strong upper-level low over southwest Kansas. Values of SRH from standard NWS rawinsonde and profiler sites over the southern Plains varied over an order of magnitude (Fig. 6a) with the largest values in southwestern Kansas, well north of the east–west boundary in Oklahoma. South (about 100 km) of this maximum, values of SRH were an order of magnitude smaller.

Focusing on the western three-quarters of Oklahoma, values of SRH ranged from about −100 to 350 m² s^{-2}
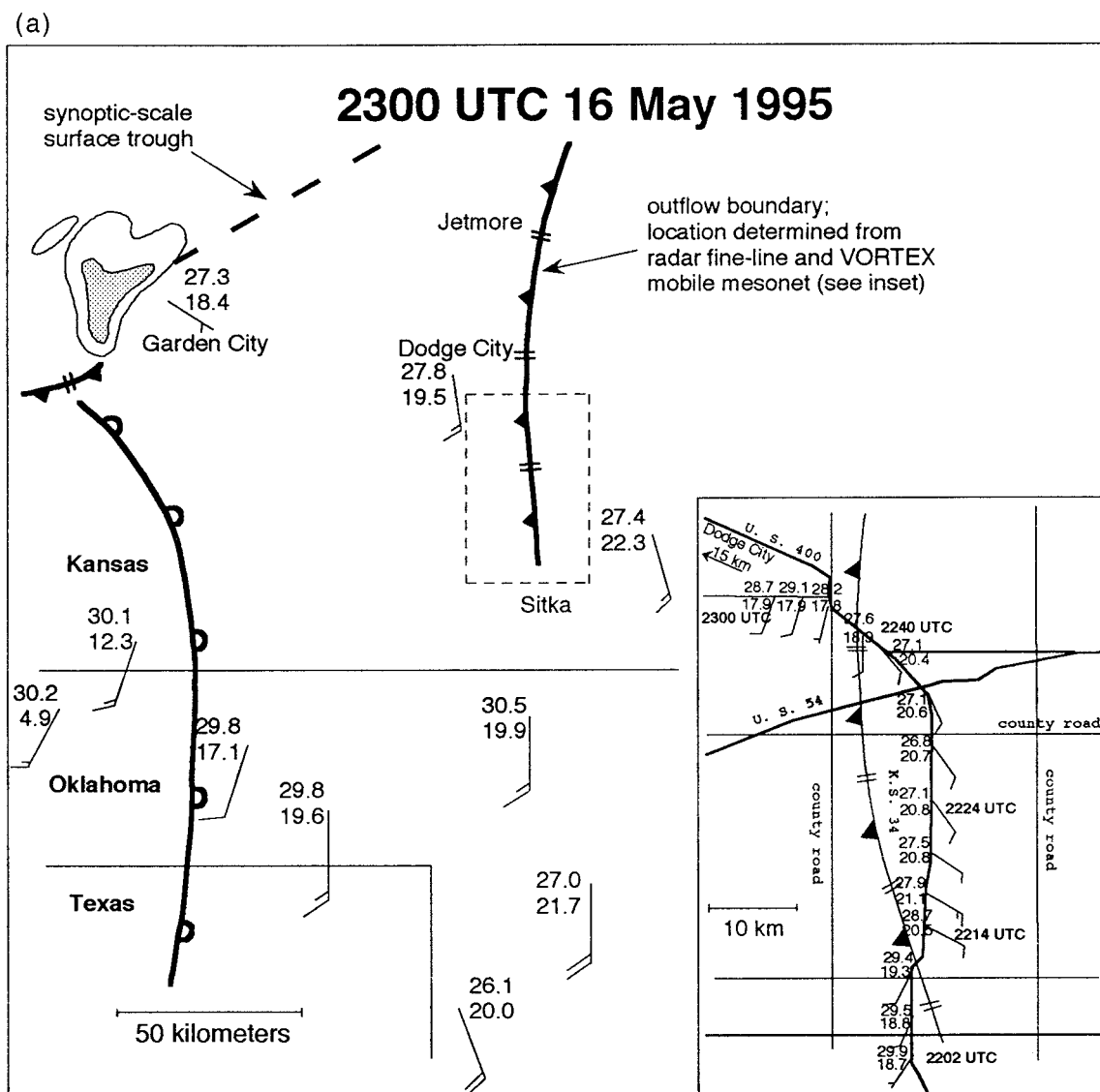
(a)

FIG. 2a. Surface mesoscale analysis for 2300 UTC 16 May 1995. Lowest tilt radar reflectivity contours of 30 and 50 dBZ are outlined (dBZ > 50 lightly shaded). Outflow boundaries are represented using the symbology of Young and Fritsch (1989). The dryline is represented by the line with unfilled scallops. Station models show temperatures and dewpoints in °C. Each full wind barb is 5 m s^{-1}, and each half-barb is 2.5 m s^{-1}. In the inset, observations from the VORTEX mobile mesonet are shown.

between about 1700 UTC 17 May 1995 and 0000 UTC 18 May 1995. Using all sites available shows at least an order of magnitude change in SRH over times of <3 h and scales less than 50–100 km (Fig. 6b). Similar to the 16–17 May 1995 case, values of shear are fairly uniform, strong, and generally supportive of supercells (Figs. 7a and 7b).

c. 2–3 June 1995

Early on 2 June 1995 convection produced a boundary detectable by satellite and radar over the Texas panhandle. A moisture gradient and this boundary both acted as a focal point for severe tornadic convection later

in the afternoon and early evening (Fig. 8a). The upper-level winds increased over a broad region from about 20 m s^{-1} at 1200 UTC to more than 40 m s^{-1} between 500 and 300 mb by 0000 UTC 3 June 1995 (Fig. 8b). The strong upper-level winds accompanied an approaching trough from the southwest. Further details of the environment evolution and the formation of 10 tornadoes are described in Richardson et al. (1998, manuscript submitted to *Mon. Wea. Rev.*).

This case shows spatial variations of SRH over the southern Plains at 0000 UTC 3 June 1995 of at least an order of magnitude or more (about −10 to 400 m^2 s^{-2}) over distances of about 100–200 km (Fig. 9a). Focusing on the Texas panhandle and extreme eastern New Mex-
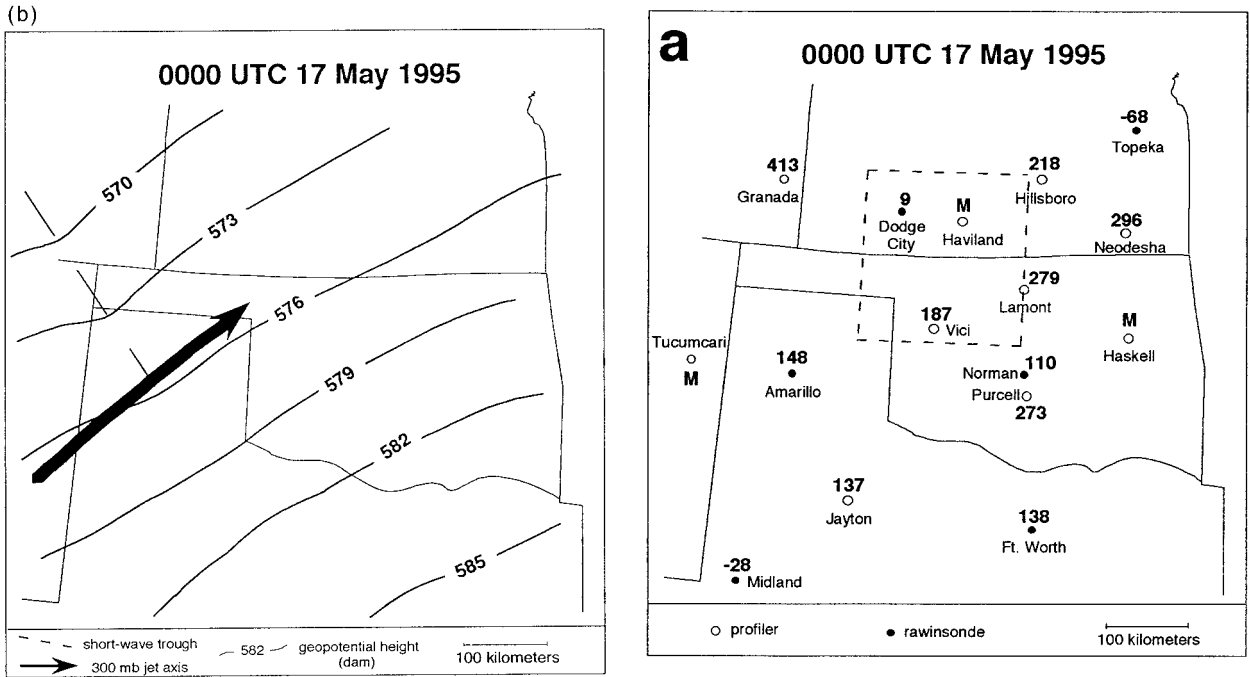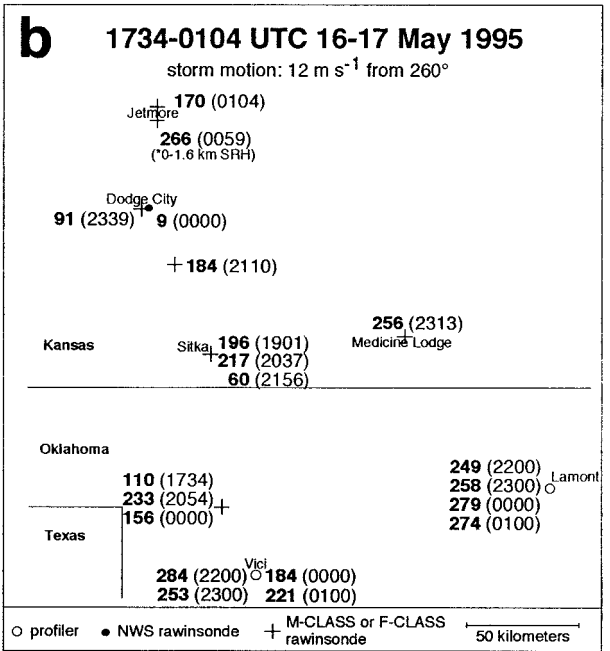
(b)

0000 UTC 17 May 1995

FIG. 2b. Analysis of 500-mb geopotential height at 0000 UTC 17 May 1995.

ico, both spatial and temporal variations changes in SRH (Fig. 9b) were as large as two orders of magnitude over short periods of time (<3 h) and short distances (<50–100 km). The largest values of SRH were found in the storm inflow of a particularly strong tornadic storm using airborne Doppler wind synthesis and mobile mesonet (inflow velocities from a mobile mesonet indicated winds at 3 m exceeded 20 m s^{-1}). Shear values, like the previous two cases, were generally strong and increased toward the west where the tornadoes occurred (Figs. 10a and 10b).

d. 8–9 June 1995

On 8–9 June 1995 21 tornadoes were reported in the Texas panhandle and extreme western Oklahoma (Fig. 11a). Several of these tornadoes were violent (≥F4) in Texas. Both low-level and upper-level winds increased dramatically between 1200 UTC 8 June 1995 and 0000 UTC 9 June 1995. The maximum upper-level jets were greater than 35 m s^{-1} (Fig. 11b shows the location of the axis of the maxima).

Similar to the other cases, SRH values varied by one

FIG. 3. SRH (0–3 km AGL) in the VORTEX domain on 16–17 May 1995. In (a), SRH at 0000 UTC 17 May is shown as sampled by the "conventional" upper-air network. The rectangular region outlined in (a) is shown in (b). In (b), SRH is shown as sampled by both the conventional network and by "unconventional" M- and F-CLASS VORTEX soundings for that event. Here "M" indicates

a   **0000 UTC 17 May 1995**

b   **1734-0104 UTC 16-17 May 1995**

that data were missing. Units of SRH are m^2 s^{-2}. The UTC times of the soundings shown in (b) appear in parentheses. Outside of the boxed region outlined in (a), SRH was computed by using the storm motion prediction technique of Rasmussen. Inside this highlighted region, SRH was computed using a mean WSR-88D-derived storm motion for that smaller area. This motion is indicated at the top of (b). Data from soundings were systematically removed at regular intervals so that sounding vertical resolution was within 50 m of the profiler vertical resolution (250 m at low levels). This was done to limit any SRH variability that may have been due to the differing vertical resolutions of the sounding data compared to the profiler data. At Neodesha, Kansas, surface data were unavailable. The surface wind at neighboring Chanute, Kansas (30 km to the northeast), was used to compute SRH.
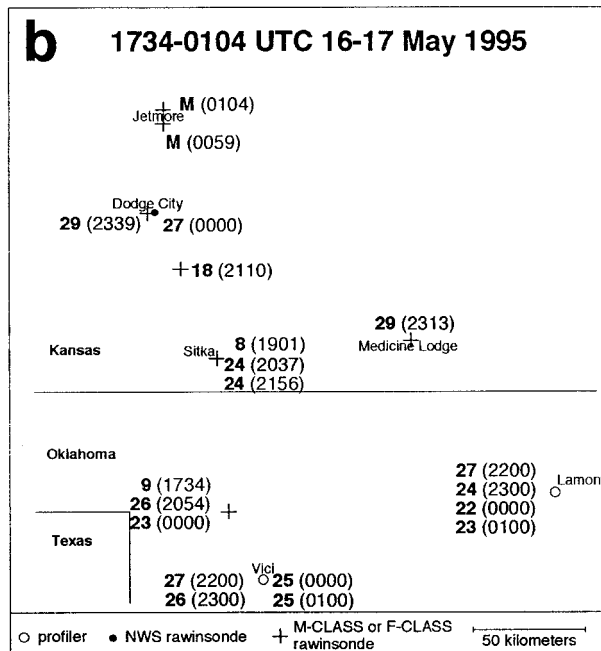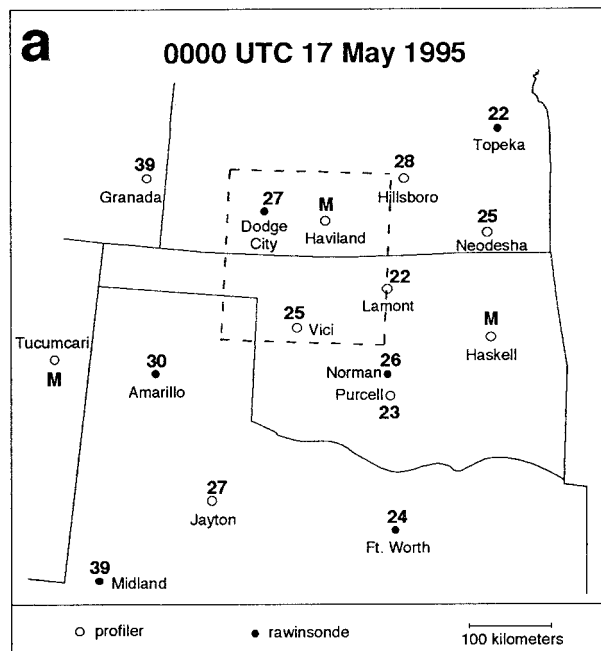
FIG. 4. Magnitude (to the nearest 1 m s^{-1}) of the shear between the lowest mean 500-m wind and the 6-km-AGL wind in the VORTEX domain on 16–17 May 1995. In (a), shear vector magnitudes at 0000 UTC 17 May are shown as sampled by the conventional upper-air network. The rectangular region outlined in (a) is shown in (b). In (b), shear vector magnitudes are shown as sampled by both the conventional network and by unconventional M- and F-CLASS VORTEX soundings for that event. Here "M" indicates that data were missing or that data were not available up to 6 km AGL. The UTC times of the soundings shown in (b) appear in parentheses. At Neodesha, Kansas, surface data were unavailable. The surface wind at neighboring Chanute, Kansas (30 km to the northeast), was used to compute the shear between the lowest mean 500-m wind and the 6-km wind.
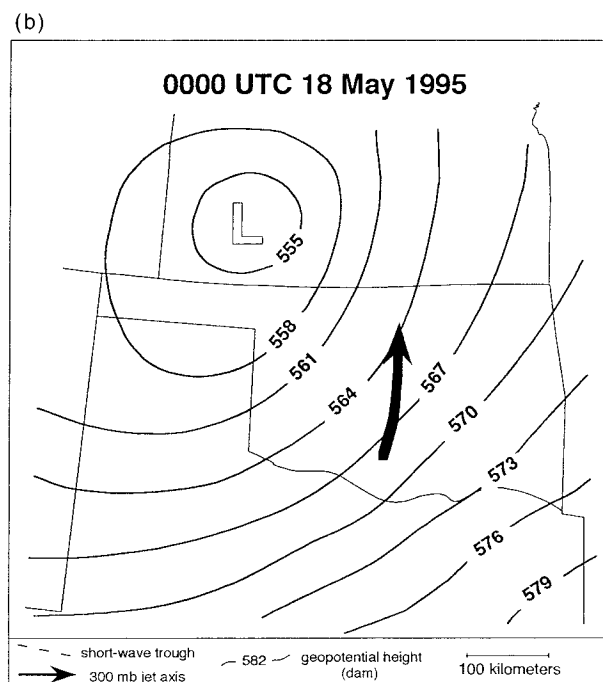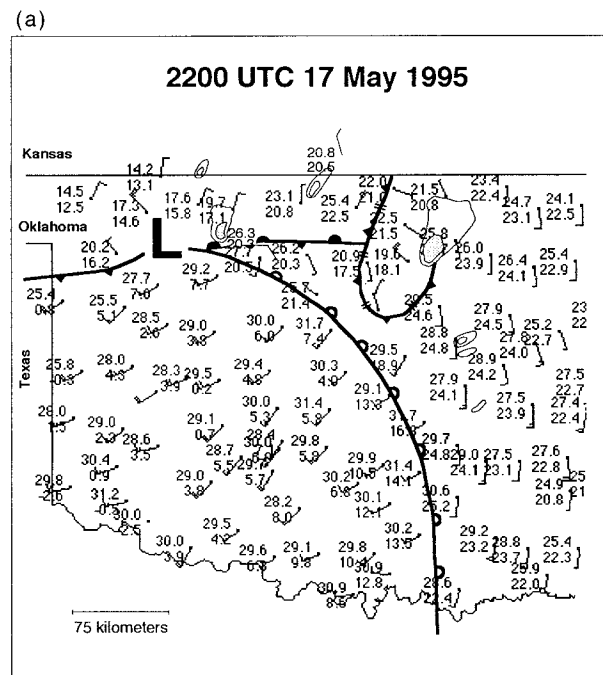
FIG. 5. (a) As in Fig. 2a but for 2200 UTC 17 May 1995. Oklahoma Mesonet data are plotted. (b) Analysis of 500-mb geopotential height at 0000 UTC 18 May 1995.

or more orders of magnitude on scales of about 100 km over the southern Plains (Fig. 12a). And like the 2–3 June 1995 case, both spatial and temporal variations in SRH (Fig. 12b) were at least two orders of magnitude over short periods of time (<3 h) and short distances (<50–100 km), especially between a thermal boundary
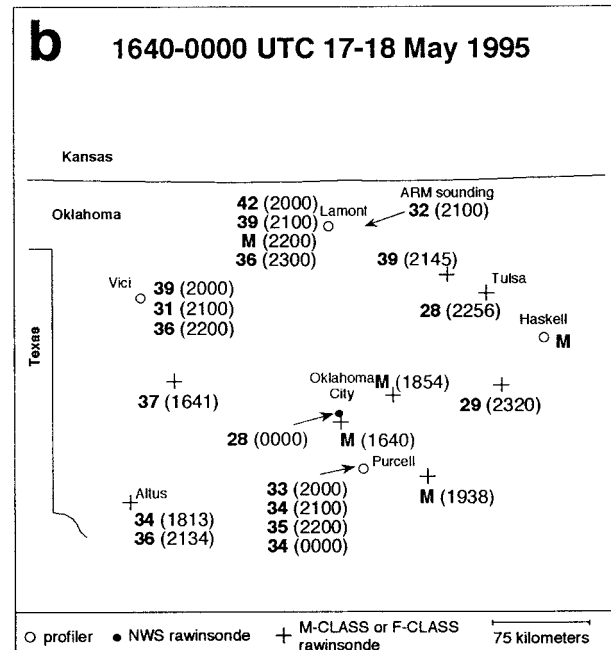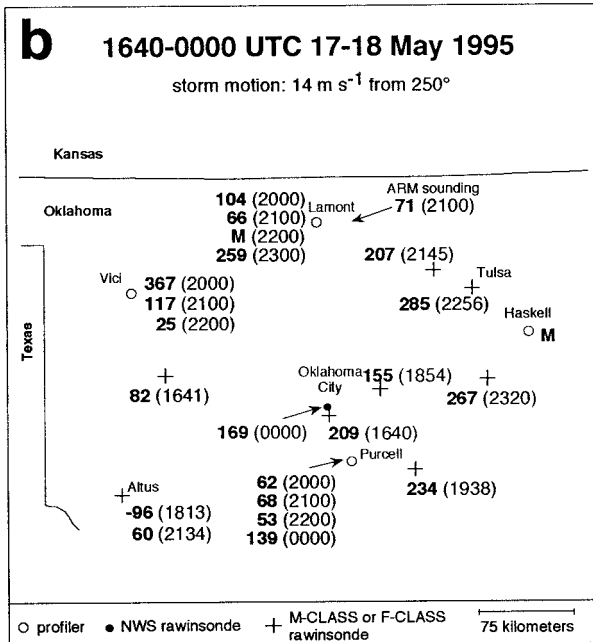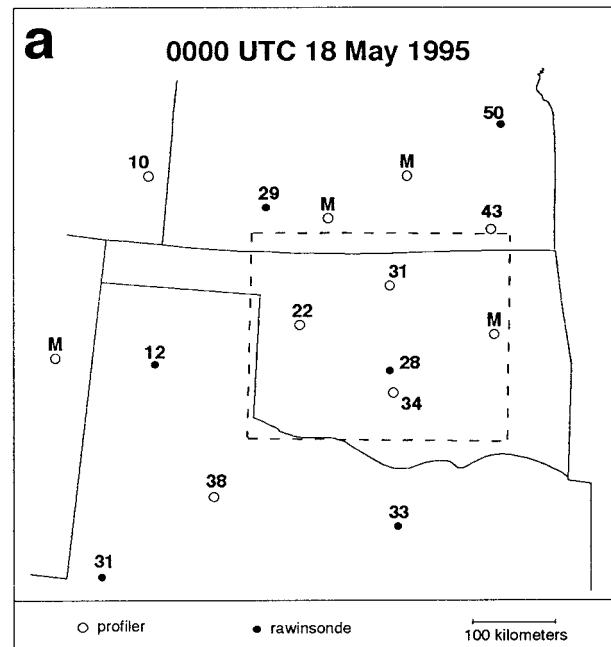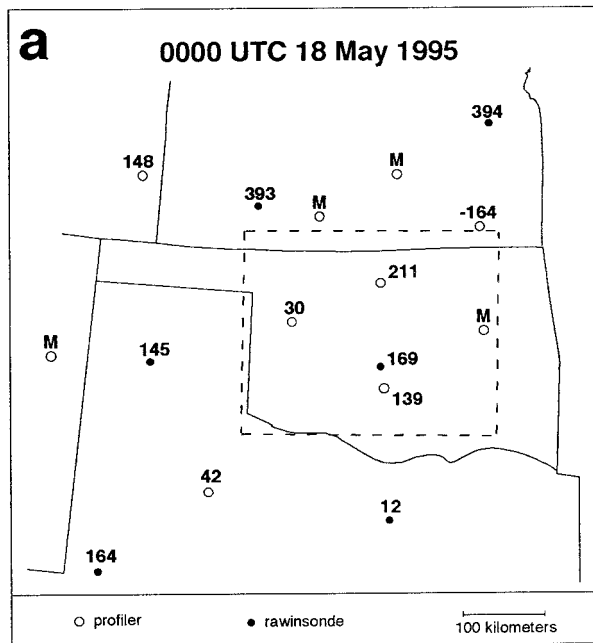
FIG. 6. As in Fig. 3 but for 17–18 May 1995. At Neodesha, Kansas, surface data were unavailable. The surface wind at neighboring Chanute, Kansas (30 km to the northeast), was used to compute SRH.

FIG. 7. As in Fig. 4, but for 17–18 May 1995. At Neodesha, Kansas, surface data were unavailable. The surface wind at neighboring Chanute, Kansas (30 km to the northeast), was used to compute the shear between the lowest mean 500-m wind and the 6-km wind.

laying over the Oklahoma panhandle and near a violent tornadic storm in the east-central Texas panhandle (inflow velocities associated with this storm as measured by a mobile mesonet indicated winds at 3 m that exceeded 25 m s^{-1}). Shear values, like the previous cases, were supportive of supercells (Figs. 13a and 13b), though not as strong as in some of the other cases (how-

ever, one sounding site in the eastern Texas panhandle indicated quite strong shear; Fig. 13b).

4. Discussion and summary

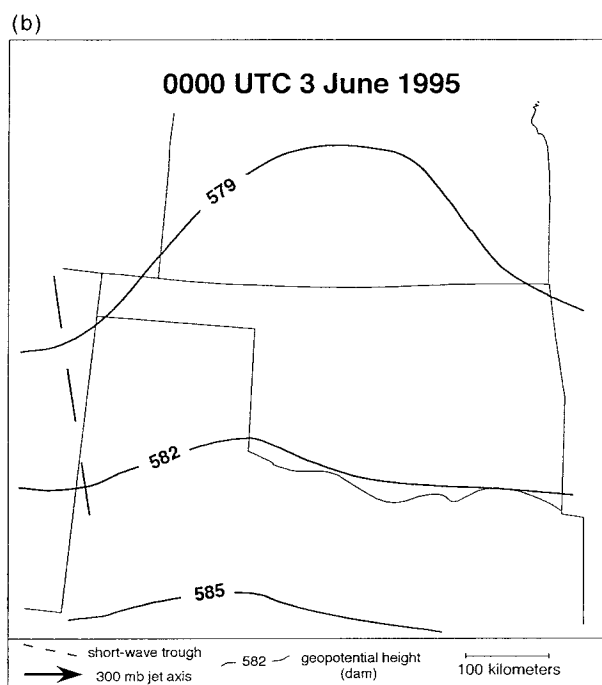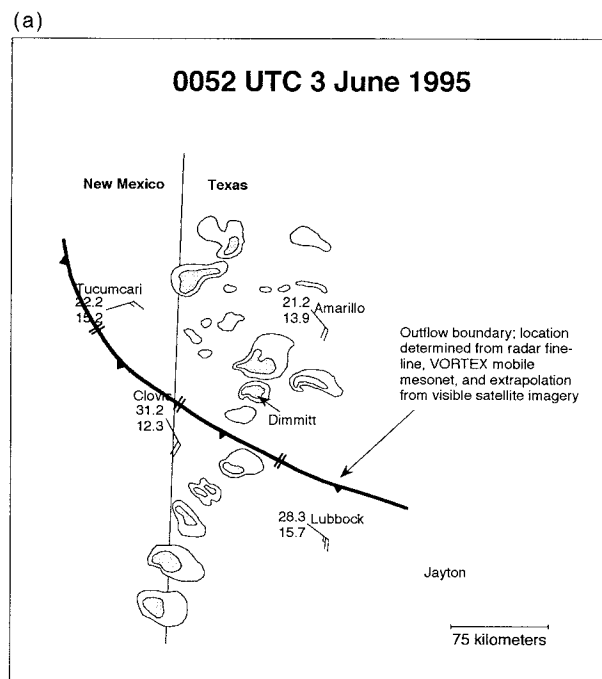It has been documented herein that SRH can have substantial variability in space (<100 km) and time (<3

(a)

(b)

FIG. 8. (a) As in Fig. 2a but for 0052 UTC 3 June 1995. (b) Analysis of 500-mb geopotential height at 0000 UTC 3 June 1995.
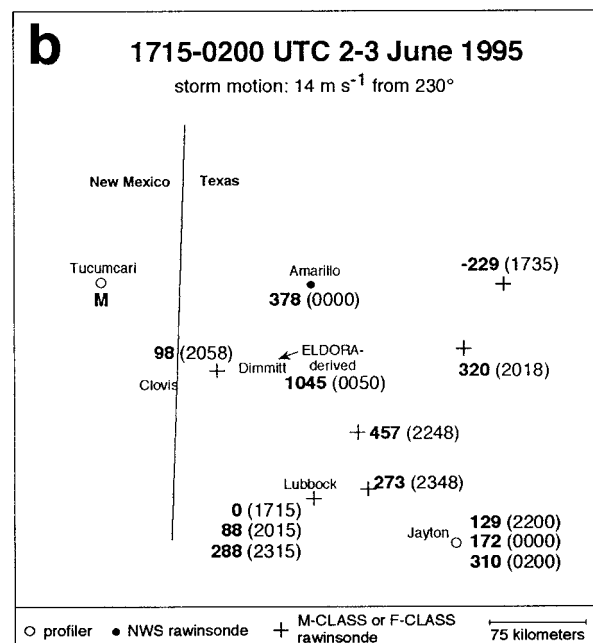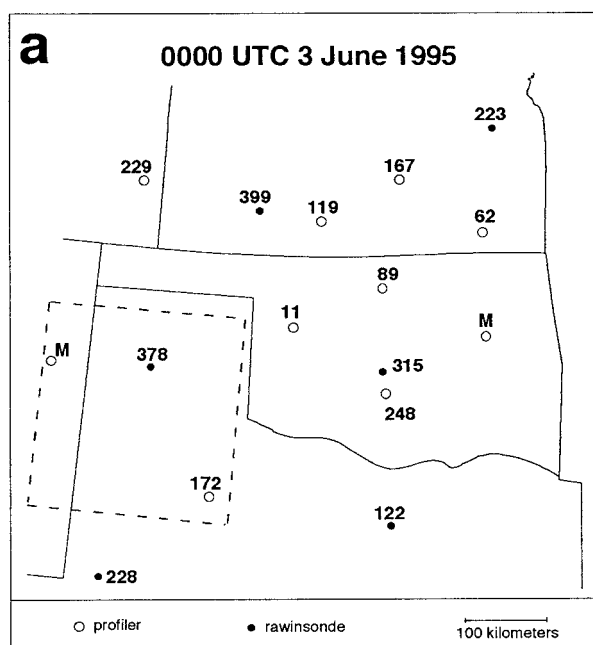

FIG. 9. As in Fig. 3 but for 2–3 June 1995. At Neodesha, Kansas, surface data were unavailable. The surface wind at neighboring Chanute, Kansas (30 km to the northeast), was used to compute SRH. Surface winds at Jayton, Texas, and Vici, Oklahoma, were also unavailable. SRH was computed at these sites using the surface winds at Lubbock, Texas (100 km west of Jayton), and Woodward, Oklahoma (30 km north of Vici), respectively.

h) where tornadoes occurred for at least the VORTEX cases investigated thus far. Variability in nontornadic and nonsupercell environments is not known for comparison. The values of SRH seem to be highly dependent on winds in the lowest levels [<1–2 km AGL; not shown for brevity's sake; however, this can be seen in works by Davies-Jones et al. (1990) and Davies-Jones

(1993)] of the atmosphere. It is believed, based on the variability of the values of SRH that were plotted here and in other studies, that there were almost certainly larger and smaller values near the various storms that developed, including those that became tornadic. The
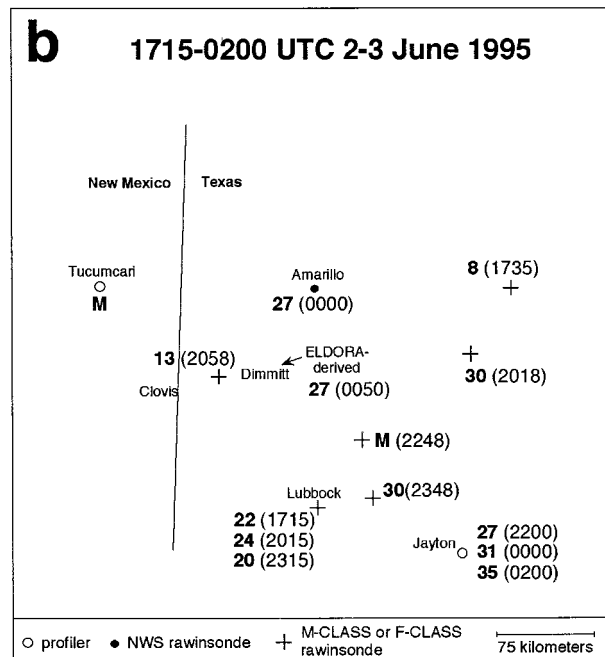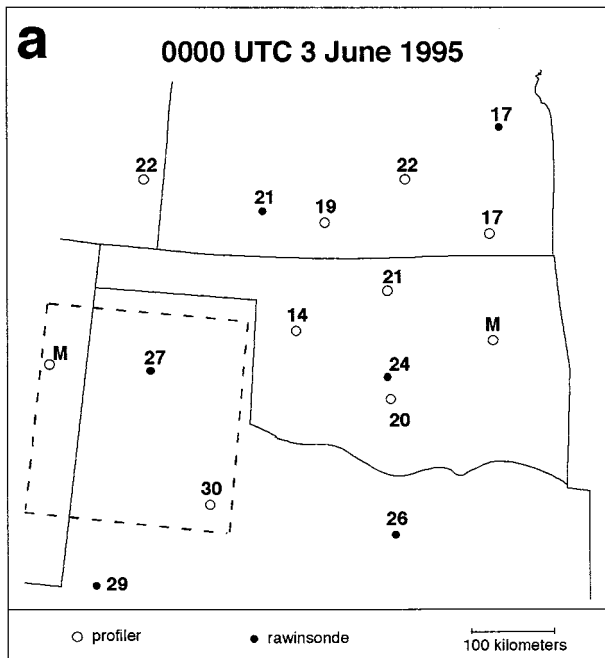
FIG. 10. As in Fig. 4 but for 2–3 June 1995. At Neodesha, Kansas, surface data were unavailable. The surface wind at neighboring Chanute, Kansas (30 km to the northeast), was used to compute the shear between the lowest mean 500-m wind and the 6-km wind.

FIG. 11. (a) As in Fig. 2a but for 0050 UTC 9 June 1995. (b) Analysis of 500-mb geopotential height at 0000 UTC 9 June 1995.

implications of this are discussed below. Another part of this work showed that the shear between the lowest mean 500-m wind and the 6-km wind was relatively uniform in all the cases in both time and space. In some cases the strongest shear was in regions where the most

intense storms occurred; however, this was not a general conclusion. From this work the following implications are suggested:

- *Important SRH variations often will not be detected.* The conventional NWS upper-air observing network does not allow for adequate sampling of variations in severe convective storm environments. It is possible

a   **0000 UTC 9 June 1995**

160 835 M 96 -11 86 198 162 441 20 241 M M 79 73 -34

○ profiler   ● rawinsonde   100 kilometers

a   **0000 UTC 9 June 1995**

24 51 M 13 18 23 19 27 9 19 19 M 14 14 23

○ profiler   ● rawinsonde   100 kilometers

b   **1700-0100 UTC 8-9 June 1995**

storm motion: 12 m s^{-1} from 220°

Oklahoma 157 (1836) Woodward 4 (1842) 7 (1823) 172 (2040)

Texas 160 (2024) 0 (1723)

179 (2026) Vici

-26 (1700) 100 (2100) 154 (2300) 94 (0100)

676 (0050) (full-resolution sounding: **1131**)

Altus

47 (2200) Jayton ○ 79 (0000)

○ profiler ● NWS rawinsonde + M-CLASS or F-CLASS rawinsonde 75 kilometers

b   **1700-0100 UTC 8-9 June 1995**

Oklahoma 20 (1836) Woodward 8 (1842) 5 (1823) 9 (2040)

Texas 14 (2024) 13 (1723)

21 (2026) Vici

12 (1700) 19 (2100) 18 (2300) 21 (0100)

35 (0050) (full-resolution sounding: **40**)

Altus

16 (2200) Jayton ○ 14 (0000)

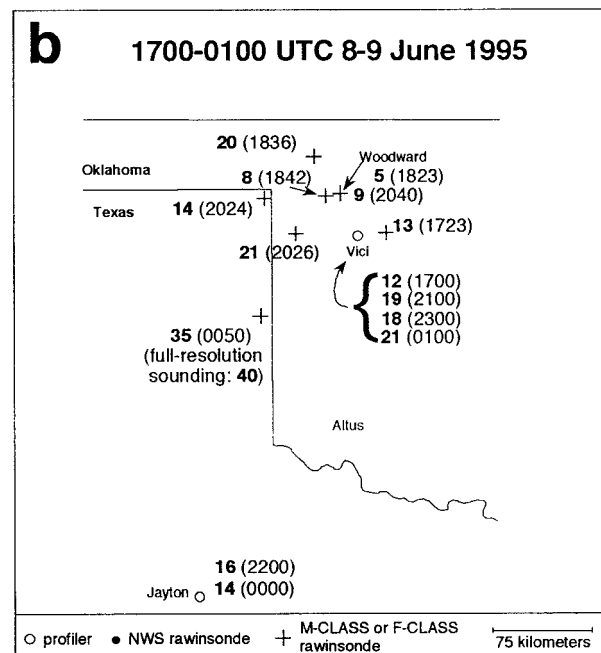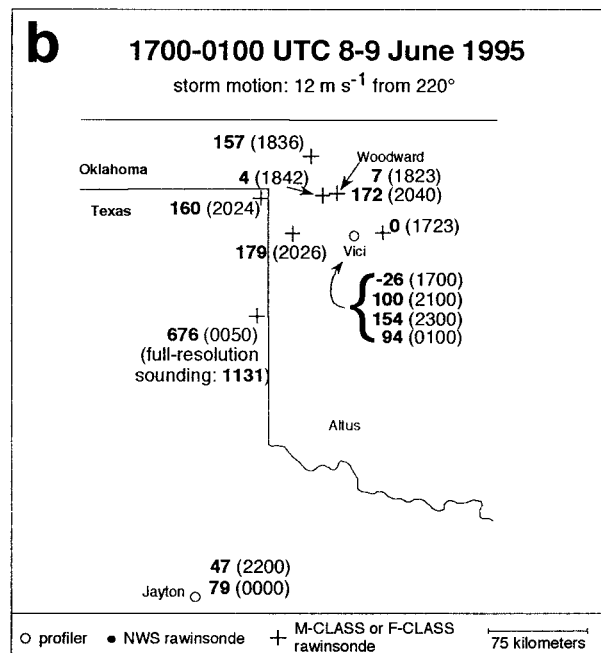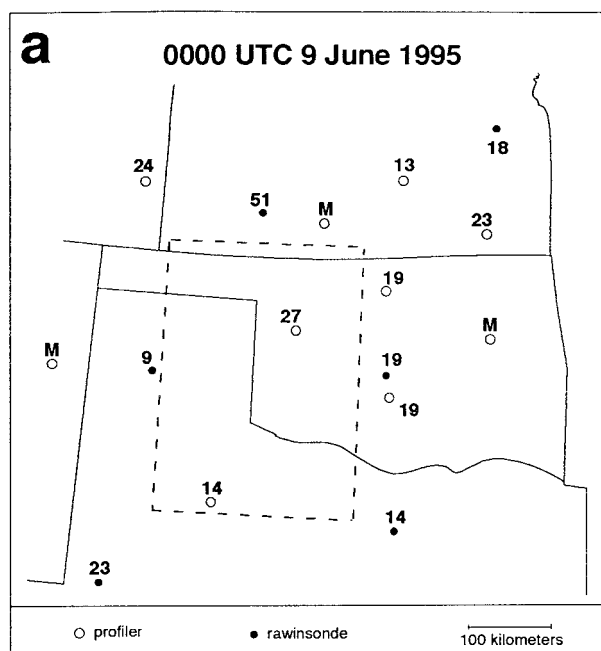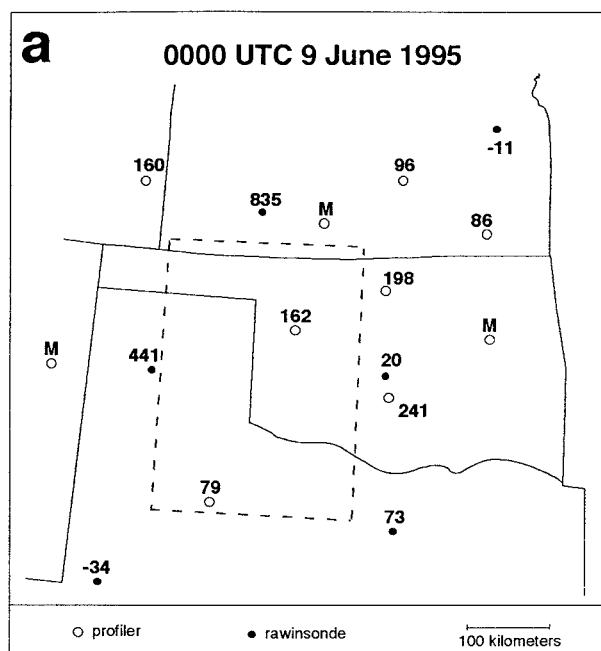○ profiler ● NWS rawinsonde + M-CLASS or F-CLASS rawinsonde 75 kilometers

FIG. 12. As in Fig. 3 but for 2–3 June 1995. At Neodesha, Kansas, surface data were unavailable. The surface wind at neighboring Chanute, Kansas (30 km to the northeast), was used to compute SRH. Surface winds at Jayton, Texas, and Vici, Oklahoma, were also unavailable. SRH values were computed at these sites using the surface winds at Lubbock, Texas (100 km west of Jayton), and Woodward, Oklahoma (30 km north of Vici), respectively.

FIG. 13. As in Fig. 4 but for 8–9 June 1995. At Neodesha, Kansas, surface data were unavailable. The surface wind at neighboring Chanute, Kansas (30 km to the northeast), was used to compute the shear between the lowest mean 500-m wind and the 6-km wind. Surface winds at Jayton, Texas, and Vici, Oklahoma, were also unavailable. The shears between the lowest mean 500-m wind and the 6 km were computed at these sites using the surface winds at Lubbock, Texas (100 km west of Jayton), and Woodward, Oklahoma (30 km north of Vici), respectively.

that careful monitoring of VAD and profilers might offer some additional guidance; however, even these are distributed over coarse scales (about 150–300 km). In the future, as more commercial aircraft are equipped to report real-time soundings of meteorological variables, including wind, potentially valuable forecast information may be available. This information will also augment calculations of low-level shear.

- *Important SRH enhancement can be anticipated near boundaries using conventional data.* If SRH is to be a useful forecast parameter, forecasters must be sensitive to the potential for highly variable SRH in regions where deep convection is occurring and boundaries are being generated. The application of a single value of SRH in a forecast in many cases may be inappropriate. Boundaries may supply additional buoyancy-generated streamwise vorticity in environments where only marginal values of SRH for severe storms are indicated.

- *Models will be of some assistance when and if they can resolve the important temporal and spatial scales for individual cases.* Mesoscale models are forever increasing resolution (now typically 30–80 km and expected to rapidly increase to 5–10 km), which should provide some guidance in primarily an ''outlook'' scenario for SRH fields. In the nowcasting arena, storm-scale prediction models (regular use of resolutions of 1–3 km will become a reality in the next five years or so) could conceivably provide some idea of variability that might indicate which storms may be important to monitor but this has yet to be demonstrated, and the limitations of these models have yet to be evaluated and established. For this to become a reality, storm initiation and evolution will need to be accurately forecast. To this date, even in high-resolution (10–50 km) mesoscale models, shear and SRH predicted in other cases tend to be smooth (e.g., Stensrud et al. 1997) compared to what was observed during VORTEX. Higher-resolution models can predict considerable varibility (sometimes as much as observed) but meaningful comparison remains an important issue in accurate storm-scale numerical weather prediction and related problems.

- *SRH variability may explain, in part, why some storms are tornadic and others are not in seemingly similar environments.* A truly enigmatic observation that has been made by almost every astute severe storm observationalist and forecaster is why one storm produces a tornado and a nearby one does not. Based on the work presented, as well as in some high-resolution (2–5-km resolution) modeling studies known to the authors, it has been shown repeatedly that SRH can be exceedingly variable. If environments with larger values of SRH are truly the ones that produce supercell tornadoes, and SRH is so variable, it might not be surprising that there is so much variability in which storms produce tornadoes. This concept needs to be more carefully investigated by examining cases where many storms produce tornadoes versus those in which only a few produce tornadoes to see if SRH was fairly uniform or highly variable in space. Also, the meaning or relevance of a threshold of SRH for supercell tornadoes needs to be more clearly defined, and how to use SRH with other important storm predictors needs to be determined.

Future work concerning the variability of SRH will involve a complete investigation of all tornadic and nontornadic supercell cases using data available from VORTEX and possibly some previous experiments (e.g., Davies-Jones et al. 1990; and Davies-Jones 1993). Furthermore, it would be interesting to know if the large heterogeneity of SRH noted for tornadic storm cases (many of which had at least one or more boundaries from one or more origins) is found in more quiescent environments. Finally, the usefulness and feasability of mesoscale and storm-scale numerical weather prediction models in resolving accurately in time and space the apparently observed heterogeneity in SRH in severe storm environments needs to be demonstrated.

REFERENCES

Bluestein, H. B., E. W. McCaul Jr., G. P. Byrd, and G. R. Woodall, 1988: Mobile sounding observations of a tornadic storm near the dryline: The Canadian, Texas storm of 7 May 1986. *Mon. Wea. Rev.,* **116,** 1790–1804.
Brock, F. V., K. Crawford, R. Elliot, G. Cuperus, S. Stadler, H. Johnson, and M. Eilts, 1995: The Oklahoma Mesonet: A technical overview. *J. Atmos. Oceanic Technol.,* **12,** 5–19.
Brooks, H. E., and R. B. Wilhelmson, 1990: The effect of low-level hodograph curvature on supercell structure. Preprints, *16th Conf. on Severe Local Storms,* Kananaskis Park, AB, Canada, Amer. Meteor. Soc., 34–39.
——, C. A. Doswell III, and R. P. Davies-Jones, 1993: Environmental helicity and the maintenance and evolution of low-level mesocyclones. *The Tornado: Its Structure, Dynamics, Prediction, and Hazards, Geophys. Monogr.,* No. 79, Amer. Geophys. Union, 97–104.
——, ——, and J. Cooper, 1994: On the environments of tornadic and nontornadic mesocyclones. *Wea. Forecasting,* **9,** 606–617.

Davies, J. M., and R. H. Johns, 1993: Some wind and instability parameters associated with strong and violent tornadoes. Part 1: Wind shear and helicity. *The Tornado: Its Structure, Dynamics, Prediction, and Hazards, Geophys. Monogr.,* No. 79, Amer. Geophys. Union, 573–582.

Davies-Jones, R. P., 1984: Streamwise vorticity: The origin of updraft rotation in supercell storms. *J. Atmos. Sci.,* **41,** 2991–3006.

——, 1993: Helicity trends in tornado outbreaks. Preprints, *17th Conf. on Severe Local Storms,* St. Louis, MO, Amer. Meteor. Soc., 56–60.

——, and H. E. Brooks, 1993: Mesocyclogenesis from a theoretical perspective. *The Tornado: Its Structure, Dynamics, Prediction, and Hazards, Geophys. Monogr.,* No. 79, Amer. Geophys. Union, 105–114.

——, D. W. Burgess, and M. Foster, 1990: Test of helicity as a forecast parameter. Preprints, *16th Conf. on Severe Local Storms,* Kananaskis Park, AB, Canada, Amer. Meteor. Soc., 588–592.

Droegemeier, K. K., S. M. Lazarus, and R. P. Davies-Jones, 1993: The influence of helicity on numerically simulated convective storms. *Mon. Wea. Rev.,* **121,** 2005–2029.

Hales, J. E., and M. D. Vescio, 1996: The March 1994 tornado outbreak in the southeast US. "The forecast process from an SPC perspective." Preprints, *18th Conf. on Severe Local Storms,* San Francisco, CA, Amer. Meteor. Soc., 32–36.

Johns, R. H., J. M. Davies, and P. W. Leftwich, 1993: Some wind and instability parameters associated with strong and violent tornadoes, Part II: Variations in the combinations of wind and stability parameters. *The Tornado: Its Structure, Dynamics, Prediction, and Hazards, Geophys. Monogr.,* No. 79, Amer. Geophys. Union, 583–590.

Klemp, J. B., and R. Rotunno, 1983: A study of the tornadic region within a supercell thunderstorm. *J. Atmos. Sci.,* **40,** 359–377.

Lauritsen, D., Z. Malekmadani, C. Morel, and R. McBeth, 1987: The Cross-chain LORAN Atmospheric Sounding System (CLASS). *Extended Abstracts, Sixth Symp. Meteorological Observations and Instrumentation.* New Orleans, LA, Amer. Meteor. Soc., 340–343.

Leftwich, P. W., 1990: On the use of helicity in operational assessment of severe local storm potential. Preprints, *16th Conf. on Severe Local Storms,* Kananaskis Park, AB, Canada, Amer. Meteor. Soc., 269–274.

Lilly, D. K., 1986a: The structure, energetics, and propagation of rotating convective storms. Part I: Energy exchange with the mean flow. *J. Atmos. Sci.,* **43,** 113–125.

——, 1986b: The structure, energetics, and propagation of rotating convective storms. Part II: Helicity and storm stabilization. *J. Atmos. Sci.,* **43,** 126–140.

Maddox, R. A., 1993: Diurnal low-level wind oscillation and storm-relative helicity. *The Tornado: Its Structure, Dynamics, Prediction, and Hazards, Geophys. Monogr.,* No. 79, Amer. Geophys. Union, 591–598.

——, L. R. Hoxit, and C. F. Chappell, 1980: A study of tornadic thunderstorm interactions with thermal boundaries. *Mon. Wea. Rev.,* **108,** 322–336.

Purdom, J. F. W., 1976: Some uses of high resolution GOES imagery in the mesoscale forecasting of convection and its behavior. *Mon. Wea. Rev.,* **104,** 1474–1483.

——, 1993: Satellite observations of tornadic thunderstorms. *The Tornado: Its Structure, Dynamics, Prediction, and Hazards, Geophys. Monogr.,* No. 79, Amer. Geophys. Union, 265–274.

Rasmussen, E. N., 1998: A climatology of severe storms in 1992. *Wea. Forecasting,* in press.

——, and R. B. Wilhelmson, 1983: Relationships between storm characteristics and 1200 GMT hodographs, low-level shear, and stability. Preprints, *13th Conf. on Severe Local Storms,* Tulsa, OK, Amer. Meteor. Soc., J5–J8.

——, J. M. Straka, R. P. Davies-Jones, C. A. Doswell III, F. H. Carr, M. D. Eilts, and D. R. MacGorman, 1994: The Verifications of the Origins of Rotation in Tornadoes Experiment: VORTEX. *Bull. Amer. Meteor. Soc.,* **75,** 997–1006.

——, Ed., and Coauthors, 1995: VORTEX—1995 operations plan. National Severe Storms Laboratory, Norman, OK, 141 pp. [Available from National Severe Storms Laboratory, Norman, OK 73069.]

Richardson, S. J., E. N. Rasmussen, J. M. Straka, P. M. Markowski, and D. O. Blanchard, 1998: The association of significant tornadoes with a baroclinic boundary on 2 June 1995. *Mon. Wea. Rev.,* in press.

Richardson, Y. P., 1993: The verification of NMC short-range models using wind profiler data. M.S. thesis, School of Meteorology, University of Oklahoma, 105 pp. [Available from School of Meteorology, University of Oklahoma, Norman, OK 73019.]

Rotunno, R., and J. B. Klemp, 1982: The influence of the shear-induced pressure gradient on thunderstorm motion. *Mon. Wea. Rev.,* **110,** 136–151.

——, and M. L. Weisman, 1988: A theory for strong, long-lived squall-lines. *J. Atmos. Sci.,* **45,** 463–485.

Rust, W. D., R. Davies-Jones, D. W. Burgess, R. A. Maddox, L. C. Showell, T. C. Marshall, and D. K. Lauritsen, 1990: Testing a mobile version of a Cross-chain LORAN Atmospheric Sounding System (M-CLASS). *Bull. Amer. Meteor. Soc.,* **71,** 173–180.

Stensrud, D. J., J. V. Cortinas Jr., and H. E. Brooks, 1997: Discriminating between tornadic and nontornadic thunderstorms using mesoscale model output. *Wea. Forecasting,* **12,** 613–632.

Straka, J. M., E. N. Rasmussen, and S. E. Frederickson, 1996: A mobile mesonet for fine-scale meteorological observations. *J. Atmos. Oceanic Technol.,* **13,** 921–936.

Weaver, J. F., and S. P. Nelson, 1982: Multiscale aspects of thunderstorm gust fronts and their effects on subsequent storm development. *Mon. Wea. Rev.,* **110,** 707–718.

Weisman, M. L., and J. B. Klemp, 1982: The dependence of numerically simulated convective storms on vertical wind shear and buoyancy. *Mon. Wea. Rev.,* **110,** 504–520.

——, and ——, 1984: The structure and classification of numerically simulated convective storms in directionally varying wind shears. *Mon. Wea. Rev.,* **112,** 2479–2498.

Young, G. S., and J. M. Fritsch, 1989: A proposal for general conventions in analysis of mesoscale boundaries. *Bull. Amer. Meteor. Soc.,* **70,** 1412–1421.

Ziegler, C. L., W. J. Martin, R. A. Pielke, and R. L. Walko, 1995: A modeling study of the dryline. *J. Atmos. Sci.,* **52,** 263–285.